Design of a Multistep Phase Mask for High-Energy Terahertz Pulse Generation by Optical Rectification

Y. Avetisyan, A. Makaryan, V. Tadevosyan & M. Tonouchi

Journal of Infrared, Millimeter, and Terahertz Waves

ISSN 1866-6892
Volume 38
Number 12

J Infrared Milli Terahz Waves (2017)
38:1439-1447
DOI 10.1007/s10762-017-0429-3

Springer

J Infrared Milli Terahz Waves (2017) 38:1439–1447
DOI 10.1007/s10762-017-0429-3

Design of a Multistep Phase Mask for High-Energy Terahertz Pulse Generation by Optical Rectification

Y. Avetisyan[1] · **A. Makaryan**[1] · **V. Tadevosyan**[1] · **M. Tonouchi**[2]

Received: 3 April 2017 / Accepted: 14 August 2017 /
Published online: 24 August 2017

Abstract A new scheme for generating high-energy terahertz (THz) pulses based on using a multistep phase mask (MSPM) is suggested and analyzed. The mask is placed on the entrance surface of the nonlinear optical (NLO) crystal eliminating the necessity of the imaging optics. In contrast to the contact grating method, introduction of large amounts of angular dispersion is avoided. The operation principle of the suggested scheme is based on the fact that the MSPM splits a single input beam into many smaller time-delayed "beamlets," which together form a discretely tilted-front laser pulse in NLO crystal. The analysis of THz-pulse generation in ZnTe and lithium niobate (LN) crystals shows that application of ZnTe crystal is more preferable, especially when long-wavelength pump sources are used. The dimensions of the mask's steps required for high-energy THz-pulse generation in ZnTe and LN crystals are calculated. The optimal number of steps is estimated, taking into account individual beamlet's spatial broadening and problems related to the mask fabrication. The proposed method is a promising way to develop high-energy, monolithic, and alignment-free THz-pulse sources.

Keywords Terahertz generation · Optical rectification · Tilted pulse-front pumping

1 Introduction

In recent years, application areas requiring intense terahertz (THz) pulses have been rapidly increasing. High-energy THz pulses are of interest for various research fields such as nonlinear spectroscopy [1, 2], material science [3, 4], and development of a new compact charged particle and x-ray sources [5, 6]. Among various methods of THz-pulse generation, the optical

✉ Y. Avetisyan
yuriav@ysu.am

[1] Microwave Engineering Department, Yerevan State University, 1 Alex Manoogian, 0025 Yerevan, Armenia

[2] Institute of Laser Engineering, Osaka University, 2-6 Yamadaoka, Suita, Osaka 565-0871, Japan

rectification (OR) in a nonlinear optical (NLO) crystal is one of the most commonly used techniques because of its simplicity and basic requirements for table-top-sized generator. In addition, it has emerged as the most powerful way to generate high-energy THz pulses, and by using a novel organic crystal DSTMS, it resulted in the highest THz pulse energy (0.9 mJ) generated to date [7]. The spectrum obtained from organic materials is typically centered in the 2 to 10 THz range, whereas THz sources with lower frequencies are needed for many applications, in particular for particle acceleration [6, 8].

The lithium niobate (LN) crystal is also an excellent material for THz generation, especially due to its high second-order nonlinear coefficient. Usually, the THz spectrum radiated by LN crystal is concentrated in the low-frequency region $\nu < 1.5$ THz. The main drawback is its inability of the collinear phase-matched THz generation due to the large difference between the THz refractive index n_{THz} and the optical group index, n_g. Generally, the phase-matched THz generation is automatically obtained in the direction determined by Cherenkov radiation angle $\theta_{Ch} = \cos^{-1}(n_g/n_{THz})$, when LN crystal is illuminated by a very narrow (as compared to the THz wavelength in the material) aperture beam. However, for powerful THz generation, wide aperture optical beams are required to escape intensity-dependent effects in LN crystal such as multiphoton absorption (MPA) at the pump wavelength and cascading nonlinear processes. For this reason, special efforts have been undertaken to compensate the phase mismatching in the beam cross-section plane.

Application of a binary phase mask in front of the LN crystal provides quasi-phase-matched (QPM) THz generation, but only in a narrow spectral bandwidth [9]. It results in increase of the THz-pulse energy, but not in increase of the THz peak power. The exclusive solution for broadband THz-pulse generation in LN crystal is application of the tilted-pulse-front pumping (TPFP) technique proposed by J. Hebling and co-workers in 2002 [10]. In a conventional setup, the pump beam is reflected off a grating to acquire a tilted-pulse-front (TPF), which is then subsequently imaged onto the crystal using a lens or a telescope. In the last decade, the TPFP technique has been continuously improved [11–14], which enabled generation of THz pulses with energy of 0.4 mJ [15] and pump-to-THz conversion efficiency $\eta = 3.8\%$ [16] in LN crystal pumped at 1030 nm wavelength. However, further increase in THz generation performance is challenging because of serious limitations [17, 18].

Significant problems inherent to the common TPFP scheme are the imaging errors in NLO crystal and the temporal broadening of the pump pulse due to the angular dispersion. Using a stair-step echelon (instead of a reflecting grating) allows obtaining discretely TPF laser pulses without degradation of the pulse duration. The generation of THz-pulses with high conversion efficiency η close to record 0.35% (at pump wavelength of 800 nm [18]) and energy of 3.1 μJ has been reported using 70 fs laser pulses at 800 nm central wavelength [19]. However, the obtained THz-pulse energy is significantly smaller than it was reported by using common TPFP technique at the same pump wavelength [18, 20]. It is related to the pump bandwidth broadening due to the cascaded nonlinearity occurring in the LN crystal [19]. Also, it is possible that imperfections in the stair-step echelon fabrication and non-optimal duration of the pump pulses reduce the generated THz-pulse energy.

To avoid problems related to the imaging errors in NLO crystal, a contact grating (CG) method has been proposed, in which a transmission grating is placed at the crystal's entrance surface [21]. Additional advantage of the CG scheme is the opportunity to use a parallel-plate form NLO crystal that eliminates the spatial non-uniformity of the interaction length. It results in a good quality THz beam and extremely high THz field in the focus of the THz-optics. Recently, this method has been realized using a thin-film contact grating deposited on LN [22]

and contact grating etched on ZnTe crystals [23]. In the experiment with LN crystal, the Yb:YAG laser pulses of 1.3 ps duration at 1030 nm wavelength were used. The generated THz-pulse energy showed a quadratic dependence on the pump laser energy, which indicates that complex phenomena such as cascade processes and multiphoton absorption did not occur. However, the THz-pulse energy was only 0.22 μJ at pump laser energy of 3.5 mJ, corresponding to a conversion efficiency of 6.3×10^{-5}.

Intense THz pulses with energy of 2.3 μJ and high conversion efficiency ~ 0.3% were generated in the experiment with ZnTe crystal thanks to pumping at an infrared wavelength sufficiently long to suppress both two- and three-photon absorptions. Besides, fabrication of CG for ZnTe crystal is relatively easy as required TPF angle is below 30°, in contrast to LN crystal, where it is about 63°. It should be noted that in CG scheme, the problems related to temporal broadening of the pump pulse are not eliminated, which can still lead to reduction of the generated THz-pulse bandwidth and energy.

In this paper, we present a new scheme of THz-pulses generation by OR in NLO crystal using multistep phase mask (MSPM) to provide discretely TPF laser pulses in the crystal. It was previously proposed and analyzed [24], but obtained results are not physically transparent; moreover, only LN crystal was considered. Here, we extend the analysis and show that application of ZnTe crystal is more preferable, especially when a longer wavelength pump source is applied. The operation principle of the MSPM is similar to that of the stair-step echelon [19]; however, MSPM works in the transmittance regime, which is beneficial for avoiding the imaging errors in the NLO crystal. In contrast to the CG method, introduction of large amount of angular dispersion in the proposed scheme is avoided as well. This is important because the optimal length of the semiconductor NLO crystals such as ZnTe or GaP can reach ~ 10 mm [23]. The abovementioned considerations indicate that the proposed scheme with MSPM attached to the NLO crystal has good potential for high-energy THz-pulses generation.

The operation principle of MSPM is illustrated in Fig. 1. The optical beam propagation through the MSPM results in the formation of an ensemble of spatiotemporal-shaped femtosecond pulses, or by other words MSPM splits a single input beam into many smaller time-delayed "beamlets," which together form an intensity front tilted with respect to the phase front.

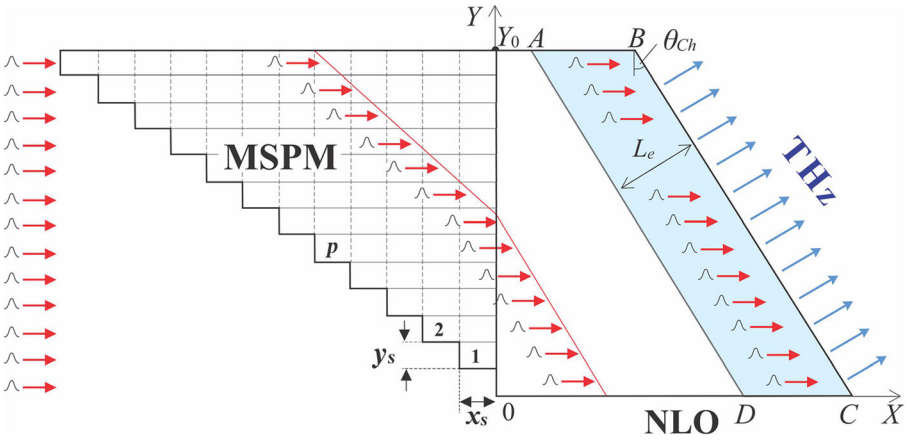

Fig. 1 Schematic view of THz generation in nonlinear optical (NLO) crystal with attached multi-step phase mask (MSPM)

2 Theoretical Considerations

It is seen from Fig. 1 that the time delay of the laser pulses propagating through every p-step of the mask is given by $\tau_p = p\tau$, where $p = 1, 2 \ldots N$ is an integer number, N is the number of the steps in MSPM, $\tau = x_s\,(n_{gm} - 1)/c$ is the delay provided by the first step $p = 1$, n_{gm} is the group index of the mask medium, x_s is the step length, and c is the speed of light. In the NLO crystal, every p-beamlet radiates a THz pulse in the form of Cherenkov wedge propagating at an angle $\theta_{Ch} = \cos^{-1}(n_g/n_{THz})$. For constructive interference of the THz pulses, certain relationship between temporal delay τ of the femtosecond pulses and beamlets distance y_s has to be satisfied. To establish that relationship, we consider a laser beam propagating through SWPM in the geometrical optics approximation having a rectangular intensity profile with the dimensions $Y_0 \times Z_0$, where $Z_0 >> Y_0$. The last inequality allows using a simple two-dimensional (2-D) theoretical model.

The analysis of THz generation in the mask covered NLO crystal [25] showed that the phase-matched THz emission at Cherenkov angle takes place, if the mask provides linearly varying delay time $\tau = y(n_{THz}\sin\theta_{Ch}/c)$. By approximating this dependence via a staircase function, we conclude that the steps thickness of MSPM and the delay time of the laser pulses have to satisfy the following Eq. (1):

$$y_s = \frac{c}{\sqrt{n_{THz}^2 - n_g^2}}\tau. \tag{1}$$

Obviously, for high-accuracy approximation, small y_s is desirable. However, to cover a certain size of the NLO crystal, large steps number N is required, complicating the MSPM fabrication. The Cherenkov-type THz emission from a separate p-beamlet is not phase-matched in the direction perpendicular to the beamlet's propagation. Using radiating antenna model [26], it has been shown that phase mismatching along the Y-axis results in reduction of the generated field by a factor $F = \mathrm{sinc}(\pi y_s/2l_c)$, where $l_c = \lambda/2n_{THz}\sin\theta_{Ch}$ is the coherence length and $\lambda = 2\pi c/\omega$ is the wavelength. In essence, the factor F indicates that THz field decrease is caused by discretely TPFP instead of a common continuous one.

Nowadays, the NLO crystals with discretely modulated nonlinear coefficient are widely used as laser radiation frequency converters [27, 28]. Due to the quasi-phase-matched (QPM) nonlinear interaction, the generated field is reduced by $\pi/2$ times in comparison with the perfectly phase-matched case. Using the same value for the F factor, we determine the steps thickness of the MSPM for the condition $y_s = y_0 \equiv l_{c0}$, where l_{c0} is the coherence length l_c at the designed (central) wavelength of THz spectrum, λ_0. Thus, the MSPM step thickness y_0 is given by

$$y_0 = \frac{\lambda_0}{2\sqrt{n_{THz}^2 - n_g^2}}. \tag{2}$$

It is instructive to note that the same Eq. (2) determines the spatial half-period of the 1-D binary mask used for QPM generation of multi-cycle THz radiation [9, 29]. The multi-cycle THz radiation was formed due to repetition of the single-cycle THz pulses (radiated by each p-beamlet), which reached to exit surface of the LN crystal with delay $\tau_p = pT_0/2$, where $T_0 = \lambda_0/c$ is the period. In our case, the 2-D MSPM introduces the same negative temporal shift

between the radiated single-cycle THz pulses, resulting in its constructive temporal overlapping.

From above, it follows that temporal delay between laser pulses propagating in the neighboring channels has to be $\tau = T_0/2$. Using $\tau = x_s\,(n_{gm} - 1)/c$, we obtain the necessary step length x_0 given by

$$x_0 = \frac{\lambda_0}{2\left(n_{gm}-1\right)}. \tag{3}$$

Thus, Eqs. (2) and (3) allow calculating both the thickness and the length of the MSPM step. From these equations, one can easily verify that in the crystal the MSPM provides discretely TPF at an angle γ equal to the Cherenkov angle θ_{Ch}. Indeed, the spatial shift of the laser pulse-fronts in the neighboring beamlets is $c\tau/n_g$ and therefore the tilt angle in the crystal is given by

$$\tan\gamma = \frac{c\tau}{y_0 n_g}. \tag{4}$$

By substituting $\tau = T_0/2$ and using Eq. (2) for y_0, one obtains that $\gamma = \theta_{Ch}$.

3 Results and Discussions

Let us now estimate the step sizes of MSPMs intended for using with LN and ZnTe crystals. The pump wavelengths are chosen respectively to be $\lambda_p = 1.7$ μm for ZnTe and $\lambda_p = 1.03$ μm for LN crystals to suppress three-photon absorption in the crystal and associated free-carrier absorption in the THz range [8, 22, 23]. For both cases, the central wavelength of the THz spectrum is chosen to be $\lambda_0 = 300$ μm.

For MSPM preparation, the materials having large group index n_{gm} are considered to realize necessary temporal delay at the shorter distances. The semiconductor materials such as GaAs and GaP seem attractive due to an opportunity of the MSPM fabrication by bonding a set of thin plates with different lengths along *X*- or *Y*-axes (see Fig. 1). The stacking techniques for GaP and GaAs plates are well developed [30–32]. However, MPA and ultrashort pulse broadening can be strong in these materials. For this reason, the wide band-gap materials such as Sapphire and GaN are preferable in using for MSPM. Hence, in the following, assuming the use of synthetic Sapphire, we set the group index to be $n_{gm} = 1.75$. The mask fabrication can be implemented by bonding technique or by etching stairs on the entrance surface.

According to Eq. (3) for chosen λ_0 and n_{gm}, the step length of the MSPM is $x_0 = 200$ μm, independent of the NLO crystal material. From Eq. (4), it follows that the required steps thicknesses of MSPM are $y_0 = 33.7$ μm and $y_0 = 98$ μm for 1.3% Mg-doped stoichiometric LN (sLN) crystal ($n_g = 2.2$ [33], $n_{THz} = 4.96$ [34]) and ZnTe crystal ($n_g = 2.79$ [35], $n_{THz} = 3.18$ [36]), respectively. Obviously, fabricating an MSPM for ZnTe crystal is easier due to larger step dimension y_0. In addition, larger y_0 is favorable for minimizing the laser beam diffraction. The Rayleigh ranges of the beamlets are $R \approx 31$ mm (6 mm) in the masks designed for ZnTe (sLN) crystals, respectively. The longest path length in the MSPM is $L_{\max} = Nx_0$, where N is the number of steps in the mask. In order to suppress the effect of the beamlets broadening, we

choose $L_{max} = R/2$, which corresponds to $N = 77$ (15) for ZnTe (sLN) crystals, respectively. Using the estimated N and the calculated values of steps sizes y_0, the effective dimensions of the NLO samples along the Y-axis are estimated to be $Y_0 = 7.5$ mm (0.47 mm) for ZnTe (sLN) crystals, respectively. Due to the opportunity of high pump power application, the THz power generated in ZnTe crystal can be significantly higher than that of sLN crystal, in spite of both, the smaller nonlinear coefficient and applicable pump intensities limited by MPA effects.

The comparative analysis of THz-pulse generation in ZnTe and LN crystals has been done in many publications [37, 38]. Some advantages of ZnTe crystal related to easier MSPM fabrication and enabling application of crystals with larger dimensions were already mentioned. However, LN crystal has about 2.5 times higher second-order nonlinear coefficient d_{eff}. In addition, in the case of ZnTe crystal, the dependence of THz-pulse energy on the pump intensity I_{av} deviates from quadratic relation above $I_{av} \approx 13.5$ GW/cm^2 [8, 23], whereas for LN crystal, the quadratic dependence holds up to $I_{av} \approx 20$ GW/cm^2 [17, 38]. For these reasons, we roughly estimate the THz pulse energy spectral density $e_{THz}(\omega)$ using radiating antenna model [26, 39] with some simplifying assumptions.

We suppose that only a portion of the crystal restricted by the area $ABCD$ is effectively involved in THz generation (Fig. 1). The effective interaction length $L_e = 1/\alpha$ is determined by the inverse value of THz-wave absorption α at designed central wavelength of THz spectrum $\lambda_{THz} = 300$ μm. The THz electrical field in far-field approximation is determined by integration of the fields generated by elementary radiators over surface of $ABCD$ area. As a result, the energy spectral density is given by

$$e_{THz}(\omega) = \left| E(\omega) \sum_{p=0}^{N} \exp\left[\frac{i\omega p \xi(\omega)}{2c}\right] \right|^2, \tag{5}$$

where $E(\omega) = Ad_{eff}L_e y_0 I_0(\omega)\mathrm{sinc}\{[n_{THz}(\omega)\cos\theta_{Ch} - n_g]\omega L_e/2c\}$ is related to THz field generated by an individual beamlet, A is the proportionality coefficient, $I_0(\omega)$ is the Fourier transform of the laser pulse intensity, and frequency depended coefficient ξ is determined by $\xi(\omega) = 2y_0\left(n_{THz}^2(\omega) - n_g^2\right)^{1/2} - \lambda_0$.

According to previous estimations, the number of steps in the MSPMs designed for ZnTe and LN crystals may be $N = 77$ and $N = 15$, respectively. However, MSPM preparation with large quantity of the steps is difficult, especially if plates bonding technique is used. For this reason, we chose $N = 30$ and $N = 15$ in the calculations of THz pulses energy densities for ZnTe and LN crystals, respectively. Figure 2 shows calculated $e_{THz}(\omega)$ using $I_0(\omega) = I_{av}\exp(-\omega^2 t^2_{im}/4)$ with $t_{im} = 225$ fs, which is related to the standard full width at half maximum (FWHM) by $\tau_s = 2(\ln 2)^{1/2} t_{im} = 375$ fs. The average intensities and interaction lengths for ZnTe (LN) crystals are chosen respectively $I_{av} = 13.5$ GW/cm^2 (20 GW/cm^2) and $L_e = 4.5$ mm (0.77 mm) using values of the absorption coefficients α given in [36] ([40]).

From Fig. 2, it follows that for ZnTe crystal, the energy spectral density at the central frequency $\nu_0 = 1$ THz is about eight times larger compared with that of LN crystal. It is mainly related to both significantly larger effective length L_e and largest possible dimension Y_0 for ZnTe crystal. From Fig. 2, it is also seen that THz spectrum generated in ZnTe crystal is slightly asymmetric relative to the central frequency of 1 THz. It is attributed to strong THz dispersion in ZnTe crystal for frequencies above 1.7 THz.

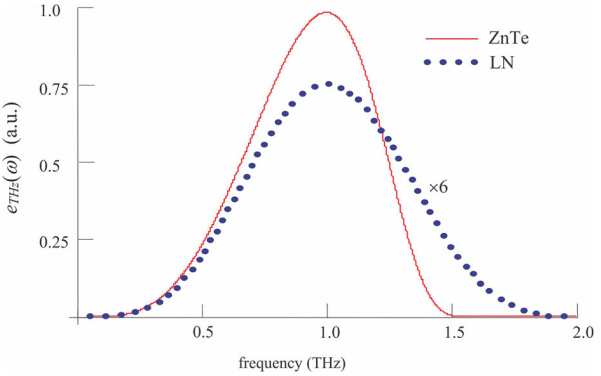

Fig. 2 Dependencies of THz pulses energy densities on frequency for ZnTe and LN crystals. In the latter case, the spectral amplitudes are multiplied by a factor of 6 for comparison clarity

4 Conclusions

In conclusion, it has been shown that the QPM generation of THz-pulses can be obtained by using a multistep phase mask contacting the entrance surface of a nonlinear crystal. The required dimensions of the mask steps were calculated for both ZnTe and LN crystals. The optimal number of steps in the mask was also estimated, taking into account individual beamlet's spatial broadening and problems related to the mask fabrication. Comparative analysis of THz-pulse generation by MSPM in ZnTe and LN crystals showed that application of ZnTe crystal is more preferable, especially when longer-wavelength laser is used as a pump source. The proposed method is a promising way to develop high-energy, monolithic, and alignment-free THz-pulse sources.

Acknowledgments This work is partially supported by State Committee of Science of Armenia (15T-6B245). The help of Dr. H. Chosrowjan is acknowledged.

References

1. J. Hebling, K.-L. Yeh, M. C. Hoffmann, and K. A. Nelson, High-power THz generation, THz nonlinear optics, and THz nonlinear spectroscopy, IEEE J. Sel. Top. Quantum Electron., vol. 14, pp. 345–353, 2008.
2. M. C Hoffmann and J. A. Fülöp, Intense ultrashort terahertz pulses: generation and applications, J. Phys. D: Appl. Phys. vol. 44, p. 083001, 2011.
3. T. Kampfrath, K. Tanaka, and K. A. Nelson, Resonant and nonresonant control over matter and light by intense terahertz transients, Nat. Photonics, vol. **7**, pp. 680–690, 2013.
4. H. Hirori, M. Nagai, and K. Tanaka, Excitonic interactions with intense terahertz pulses in ZnSe/ZnMgSSe multiple quantum wells, Phys. Rev. B., vol. 81, p. 081305, 2010.
5. L. Pálfalvi, J. A. Fülöp, Gy. Tóth, and J. Hebling, Evanescent-wave proton post accelerator driven by intense THz pulse, Phys. Rev. ST Accel. Beams., vol. 17, p. 031301, 2014.
6. E. A. Nanni, W. R. Huang, K.-H. Hong, K. Ravi, A. Fallahi, G. Moriena, R. J. D. Miller, and F. X. Kärtner, Terahertz-driven linear electron acceleration, Nat. Commun., vol. 6, p. 8486, 2015.
7. C. Vicario, A. V. Ovchinnikov, S. I. Ashitkov, M. B. Agranat, V. E. Fortov, and C. P. Hauri, Generation of 0.9-mJ THz pulses in DSTMS pumped by a Cr:Mg_2SiO_4 laser, Opt. Lett. vol. 39, pp. 6632–6635, 2014.
8. G. Polónyi, B. Monoszlai, G. Gäumann, G. Andriukaitis, T. Balciunas, A. Pugzlys, A. Baltuska, T. Feurer, J. Hebling, and J. A. Fülöp, High-energy terahertz pulses from semiconductors pumped beyond the three-photon absorption edge, Opt. Express, vol. 24, pp. 23872–23882, 2016.

9. C. Zhang, Y. Avestisyan, G. Abgaryan, I. Kawayama, H. Murakami, and M. Tonouchi, Tunable narrowband terahertz generation in lithium niobate crystals using a binary phase mask, Opt. Lett., vol. 38, pp. 953–955, 2013.
10. J. Hebling, G. Almási, I. Z. Kozma, and J. Kuhl, Velocity matching by pulse front tilting for large-area THz-pulse generation, Opt. Lett., vol. 10, pp. 1161–1166, 2002.
11. K-L Yeh, M C Hoffmann, J Hebling, K A Nelson, Generation of 10 μJ ultrashort THz pulses by optical rectification, Appl. Phys. Lett., vol. 90, 171121, 2007.
12. H Hirori, A Doi, F Blanchard, K Tanaka. Single-cycle terahertz pulses with amplitudes exceeding 1 MV/cm generated by optical rectification in LiNbO3, Appl. Phys. Lett. vol. 98, 091106, 2011.
13. M. Nagai, E. Matsubara, and M. Ashida, High-efficiency terahertz pulse generation via optical rectification by suppressing stimulated Raman scattering process, Opt. Express, vol. 20, pp. 6509–6514, 2012.
14. X. Wu, A.-L. Calandron, K. Ravi, C. Zhou, M. Hemmer, F. Reichert, D. Zhang, H. Cancaya, L. Zapata, N. Matlis, and F. Kartner, Optical generation of single-cycle 10 MW peak power 100 GHz waves, Opt. Express, vol. 24, pp. 21059–21069, 2016.
15. J. A. Fülöp, Z. Ollmann, C. Lombosi, C. Skrobol, S. Klingebiel, L. Pálfalvi, F. Krausz, S. Karsch, and J. Hebling, Efficient generation of THz pulses with 0.4 mJ energy, Opt. Express, vol. 22, pp. 20155–20163, 2014.
16. S.-W. Huang, E. Granados, W. R. Huang, K.-H. Hong, L. E. Zapata, and F. X. Kärtner, High conversion efficiency, high energy terahertz pulses by optical rectification in cryogenically cooled lithium niobate, Opt. Lett., vol. 38, pp. 796–798, 2013.
17. K. Ravi, W. R. Huang, S. Carbajo, X. Wu, and F. X. Kärtner, Limitations to THz generation by optical rectification using tilted pulse fronts, Opt. Express, vol. 22, pp. 20239–20251, 2014.
18. F. Blanchard, X. Ropagnol, H. Hafez, H. Razavipour, M. Bolduc, R. Morandotti, T. Ozaki, and D. G. Cooke, Effect of extreme pump pulse reshaping on intense terahertz emission in lithium niobate at multimilli Joule pump energies, Opt. Lett., vol. 39, pp. 4333–4336, 2014.
19. B. Ofori-Okai, P. Sivarajah, W. Huang, and K. Nelson, THz generation using a reflective stair-step echelon, Opt. Express, vol. 24, pp. 5057–5068, 2016.
20. S. Zhong, Ju. Li, Z. Zhai, L. Zhu, Ji. Li, P. Zhou, J. Zhao, and Ze. Li, Generation of 0.19-mJ THz pulses in $LiNbO_3$ driven by 800-nm femtosecond laser, Opt. Express, vol. 24, pp. 14828–14835, 2016.
21. L. Palfalvi, J. A. Fülöp, G. Almasi, and J. Hebling, Novel setups for extremely high power single-cycle terahertz pulse generation by optical rectification, Appl. Phys. Lett., vol. 92, p. 171107, 2008.
22. F. Yoshida, K. Nagashima, M. Tsubouchi, M. Maruyama, and Y. Ochi, THz pulse generation using a contact grating device composed of TiO2/SiO2 thin films on LiNbO3 crystal, J. Appl. Phys., vol. 120, p. 183103, 2016.
23. J. A. Fülöp, G. Polónyi, B. Monoszlai, G. Andriukaitis, T. Balciunas, A. Pugzlys, G. Arthur, A. Baltuska, and J. Hebling, Highly efficient scalable monolithic semiconductor terahertz pulse source, Optica, vol. 3, pp. 1075–1078, 2016.
24. G. Abgaryan, A. Makaryan, V. Tadevosyan, and Y. Avetisyan, Broadband THz generation in lithium niobate crystal by step-wise phase mask, in Proceedings of Microwave and THz Technique and Applications ("Gitutiun" Publishing House of the NAS RA Yerevan 2015), pp. 13–16. http://irphe.asjoa.am/85/5/IRPhE2014_Proceedings.pdf.
25. Y. Avetisyan, M. Tonouchi, Terahertz generation in QPM structure formed by a phase mask, Opt. Lett., vol. 37, pp. 4155–4157, 2012.
26. J. L'huillier, G. Torosyan, M. Theuer, Y. Avetisyan, and R. Beigang, Generation of THz radiation using bulk, periodically and aperiodically poled lithium niobate—Part 1: Theory, Appl. Phys. B., vol. 86, pp. 185–196, 2007.
27. K. L. Vodopyanov, Optical THz-wave generation with periodically-inverted GaAs, Laser & Photon. Rev., vol. 2, pp. 11–25, 2008.
28. M. M. Fejer, G. A. Magel, D. H. Jundt, and R. L. Byer, Quasi-phase-matched second harmonic generation: tuning and tolerances, IEEE J. Quantum Electron., vol. 28, pp. 2631–2654, 1992.
29. Y. Avestisyan, C. Zhang, I. Kawayama, H. Murakami, T. Somekawa, H. Chosrowjan, M. Fujita, and M. Tonouchi, Terahertz generation by optical rectification in lithium niobate crystal using a shadow mask, Opt. Express, vol. 20, pp. 25752–25757, 2012.
30. Y. Jiang, D. Li, Y. J. Ding, and I. B. Zotova, Terahertz generation based on parametric conversion: from saturation of conversion efficiency to back conversion, Opt. Lett., vol. 36, pp. 1608–1610, 2011.
31. D. Zheng, L. A. Gordon, Y. S. Wu, R. S. Feigelson, M. M. Fejer, R. L. Byer, and K. L. Vodopyanov, 16-μm infrared generation by difference frequency mixing in diffusion-bonded-stacked GaAs, Opt. Lett., vol. 23, pp. 1010–1012, 1998.
32. T. Kubota, H. Atarashi, and I. Shoji, Fabrication of quasi-phase-matching stack of GaAs plates using a new technique: room-temperature bonding, in Advanced Solid-State Lasers, OSA Technical Digest Series (online) (Optical Society of America, 2016), paper ATu5A.6. https://www.osapublishing.org/abstract.cfm?uri=ASSL-2016-ATu5A.6.

33. O. Gayer, Z. Sacks, E. Galun, and A. Arie, Temperature and wavelength dependent refractive index equations for MgO-doped congruent and stoichiometric $LiNbO_3$, Appl. Phys. B., vol. 91, pp. 343–348, 2008.
34. L. Palfalvi, J. Hebling, J. Kuhl, A. Peter, and K. Polgar, Temperature dependence of the absorption and refraction of Mg-doped congruent and stoichiometric LiNbO3 in the THz range, J. Appl. Phys., vol. 97, p. 123505, 2005.
35. D. T. F. Marple, Refractive index of ZnSe, ZnTe, and CdTe, J. Appl. Phys., vol. 35, pp. 539–541, 1964.
36. S. R. Tripathi, M. Aoki, M. Takeda, T. Asahi, I. Hosako and N. Hiromot, Accurate complex refractive index with standard deviation of ZnTe measured by terahertz time domain spectroscopy, Jap. J. Appl. Phys., vol. 52, p. 042401, 2013.
37. J. A. Fülöp, L. Pálfalvi, G. Almási, and J. Hebling, Design of high-energy terahertz sources based on optical rectification, Opt. Express, vol. 18, pp. 12311–12327, 2010.
38. M. C. Hoffmann, K.-L. Yeh, J. Hebling, and K. A. Nelson, Efficient terahertz generation by optical rectification at 1035 nm, Opt. Express, vol. 15, pp. 11706–11713, 2007.
39. Y. Avetisyan, C. Zhang, and M. Tonouchi, Analysis of linewidth tunable terahertz wave generation in periodically poled lithium niobate, J. Infrared Milli. Terahz Waves, vol. 33, pp. 989–998, 2012.
40. M. Unferdorben, Z. Szaller, I. Hajdara, J. Hebling & L. Pálfalvi, Measurement of refractive index and absorption coefficient of congruent and stoichiometric lithium niobate in the terahertz range, J. Infrared Milli Terahz Waves, vol. 36, pp. 1203–1209, 2015.